Boosting tumor homing of endogenous natural killer cells via therapeutic secretomes of chemically primed natural killer cells

Seohyun Cho, Seung Hee Choi [ORCID], Eunchong Maeng, Hail Park, Ki Seo Ryu, Kyung-Soon Park [ORCID]

Division of life science, Department of Biomedical Science, CHA University, Seongnam-si, Korea (the Republic of)

Correspondence to
Professor Kyung-Soon Park; kspark@cha.ac.kr

ABSTRACT

Background Natural killer (NK) cells play a critical role in modulating immune responses by secreting soluble factors, including chemotactic cytokines. Our previous study demonstrated the potent antitumor activity of Chem_NK, referring to NK cells chemically primed with 25 kDa branched polyethyleneimine. However, the potential of Chem_NK secretomes to educate other NK cells and enhance their tumor-homing ability remains unexplored.

Methods The effects of Chem_NK conditioned media (Chem CM) on NK cells were evaluated in vitro by examining chemokine receptor expression and migration toward cancer cells. In vivo, the impact of Chem_NK and Chem CM on endogenous NK cell populations was assessed using xenograft and syngeneic mouse tumor models. Cytokine array and signaling analyses were performed to identify factors secreted by Chem_NK and their role in activating recipient NK cells.

Results Chem CM effectively educated NK cells in vitro, enhancing chemokine receptor expression and improving their migration toward cancer cells. In vivo, adoptively transferred Chem_NK increased endogenous NK cell populations within xenograft tumors. Furthermore, direct injection of Chem CM into a syngeneic mouse tumor model significantly promoted endogenous NK cell infiltration into tumors and suppressed lung metastasis. Cytokine analysis revealed that Chem_NK secreted high levels of cytokines, which activated ERK1/2 signaling in recipient NK cells, leading to upregulation of chemokine receptors.

Conclusions Chem_NK secretomes effectively enhance the tumor-homing ability of NK cells and amplify antitumor efficacy by educating other NK cells. These findings offer novel insights into activated NK cell-mediated immune communication and highlight the therapeutic potential of NK cell-derived secretomes in cancer therapy.

WHAT IS ALREADY KNOWN ON THIS TOPIC

⇒ Natural killer (NK) cells can be chemically primed ex vivo with 25 kDa branched polyethyleneimine to exhibit enhanced antitumor activity. This priming approach effectively boosts the cytotoxic potential of NK cells against ovarian and triple-negative breast cancer model in mice.

WHAT THIS STUDY ADDS

⇒ Chemically primed NK cells' secretomes have the ability to modulate other NK cells, enhancing their migratory capacity toward tumor sites. This interaction significantly improves the therapeutic efficacy of NK cell-based treatments.

HOW THIS STUDY MIGHT AFFECT RESEARCH, PRACTICE OR POLICY

⇒ This study underscores the novel role of activated NK cell secretomes in modulating other NK cells, providing a potential avenue for developing immunotherapy strategies such as therapeutic cancer vaccines or adjuvants.

INTRODUCTION

Natural killer (NK) cells play a crucial role in the body's initial immune defenses, constituting approximately 5–15% of the total peripheral lymphocyte population.[1] NK cells rapidly target infected or malignant cells without prior sensitization, using mechanisms like perforin and granzymes for cytotoxicity. Alternatively, they can use secreted effector molecules belonging to the tumor necrosis factor (TNF) family, such as TNF, TNF-related apoptosis-inducing ligand, and Fas ligand.[2]

Numerous studies have highlighted the correlation between impaired NK cell cytotoxic activity and an elevated risk of cancer.[3] Given the instrumental role of NK cells in performing immune surveillance, actively monitoring hematological malignancies and solid tumors, and preventing metastatic spread,[4–6] this underscores the potential to harness NK cell functions for more effective cancer management.

In line with this, clinical trials have shown promising results for CD19-targeted chimeric antigen receptor (CAR)-NK therapy in B-cell malignancies, garnering attention for NK cell therapy.[7 8] The next challenge in cancer immunotherapy is addressing solid tumors.

Despite the relatively low density of NK cells compared with CD8^{+} T cells and macrophages,[9 10] clinical data suggest that NK cell infiltration into tumors is a positive prognostic marker for several cancers like lung and breast cancer.[11–13] Systematic reviews and meta-analyses have consistently demonstrated that NK cell infiltration into solid tumors is associated with improved overall survival in cases.[14] Consequently, enhancing the trafficking capacity of NK cells to solid tumors is a key challenge to improve the effectiveness of NK cell therapy against solid tumors.[15]

Gaining insight into the mechanisms that influence the expression of receptors associated with migration and their corresponding ligands is crucial to enhance the infiltration of NK cells into solid tumors. NK cells migrate to various target tissues, and this is mediated by a family of secreted chemokines.[16] Although evidence on cytokines direct impact on NK cell homing in vivo is insufficient, cytokines, either individually or in combination, elicit significant and varied effects on chemokine receptor profiles in vitro. For example, incubation of human primary NK cells with interleukin (IL)-2 in conjunction with IL-12, IL-15, or IL-18 enhances expression of chemokine receptors such as CCR1, CCR7, and CXCR6, leading to improved NK cell migration.[17–20] Although NK cells can secrete cytokines and other factors, our understanding of the activity of their secretome is limited. Given that NK cells produce chemokines and cytokines on activation to eliminate tumors and control metastasis,[21 22] broadening our comprehension of the biological activities of secretome by NK cells could reveal new opportunities for NK cell-based cancer immunotherapy.

We previously demonstrated that NK cells can be primed for potent antitumor activity using 25 kDa branched polyethyleneimine (25KbPEI) and referred to these chemically primed NK cells as Chem_NK.[23] Building on our previous study, which identified enhanced production of interferon (IFN)-γ as one of the notable phenotypes of Chem_NK,[24] we hypothesized that Chem_NK secrete additional molecules with immunological activity. Indeed, the present study demonstrates that Chem_NK secrete a significant quantity of molecules that enhance the migration abilities of recipient NK cells toward cancer cells in vitro and improve the tumor infiltration capacity of endogenous NK cells in vivo. Our findings provide evidence that secretomes of Chem_NK educate other NK cells by activating the ERK signaling pathway, resulting in increased expression of chemokine receptors.

RESULTS
Chem_NK recruit other NK cells
Previously, we reported that Chem_NK possess potent antitumor activity and an enhanced tumor infiltration capability in both ovarian and breast cancers.[23] Given that Chem_NK produces a substantial amount of IFN-γ, which enhances the antitumor activity of NK cells,[25] we questioned whether they can also educate other NK cells. To investigate this, we established a PC-3 xenograft model

in nude mice, administered control NK cells (C_NK) or Chem_NK intravenously, and then analyzed the tumor-homing activity of endogenous NK cells (figure 1A). As anticipated, mice injected with Chem_NK showed increased tumor infiltration by endogenous NK cells compared with those injected with C_NK (figure 1B). Given the enhanced tumor infiltration capability of Chem_NK, the observed increase in endogenous NK cells within the tumor can be attributed to the presence of Chem_NK in the tumor. Therefore, we conducted a transwell assay and assessed the migration of NK-92MI cells from the upper chamber toward C_NK or Chem_NK in the lower chamber. More NK-92MI cells migrated toward Chem_NK than toward C_NK (figure 1C). To confirm that the improved trafficking of NK cells is mediated by the secreted molecules of Chem_NK, we next examined the migration of NK-92MI cells toward the conditioned media (CM) of C_NK and Chem_NK (online supplemental figure 1). Consistent with the result presented in figure 1C, more NK-92MI cells migrated toward CM of Chem_NK (Chem CM) than toward CM of C_NK (C CM) (figure 1D). These results indicate that Chem_NK produce more chemoattractant molecules than C_NK.

Chem CM promotes the migration of NK cells toward tumors
While figure 1D indicates that more NK cells migrated toward Chem CM, it remained unclear whether Chem CM attracts NK cells by enhancing their migration to cancer cells. We incubated NK-92MI cells in Chem CM for 24 hours (Chem CM_NK) and then evaluated their migration toward cancer cells (figure 2A). The migration ability of Chem CM_NK toward cancer cells was significantly better than that of NK-92MI cells incubated in C CM (C CM_NK) (figure 2B).

To evaluate the efficacy of Chem CM in promoting in vivo endogenous NK cell migration, we first administered Chem CM intraperitoneally for 3 days, followed by an orthotopic injection of EO771 cells into nude mice (figure 2C). At 17 days post-implantation, we dissected the tumors for quantitative analysis of infiltrating NK cells. After initially gating total cells for mCD45^{+} cells, t-distributed stochastic neighbor embedding (t-SNE) analysis was performed to cluster NK cells. This analysis revealed there was an increased population of mNKp46^{+} cells within the mCD45^{+} cell population in tumors from Chem CM group compared with the C CM and Dulbecco's phosphate-buffered saline (DPBS) groups (figure 2D). Consistently, the percentage of mNKp46^{+} cells among mCD45^{+} cells was significantly higher in tumors from the Chem CM group than in those from the C CM and DPBS groups (figure 2E). Additionally, immunofluorescence staining of tumor sections revealed the notable presence of tumor-infiltrated NK cells in the Chem CM group (figure 2F). Taken together, these in vivo findings suggest that Chem CM contains secretomes that enhance the tumor-homing ability of NK cells and that endogenous mouse NK cells are primed by Chem CM, thereby improving their migration toward tumors.
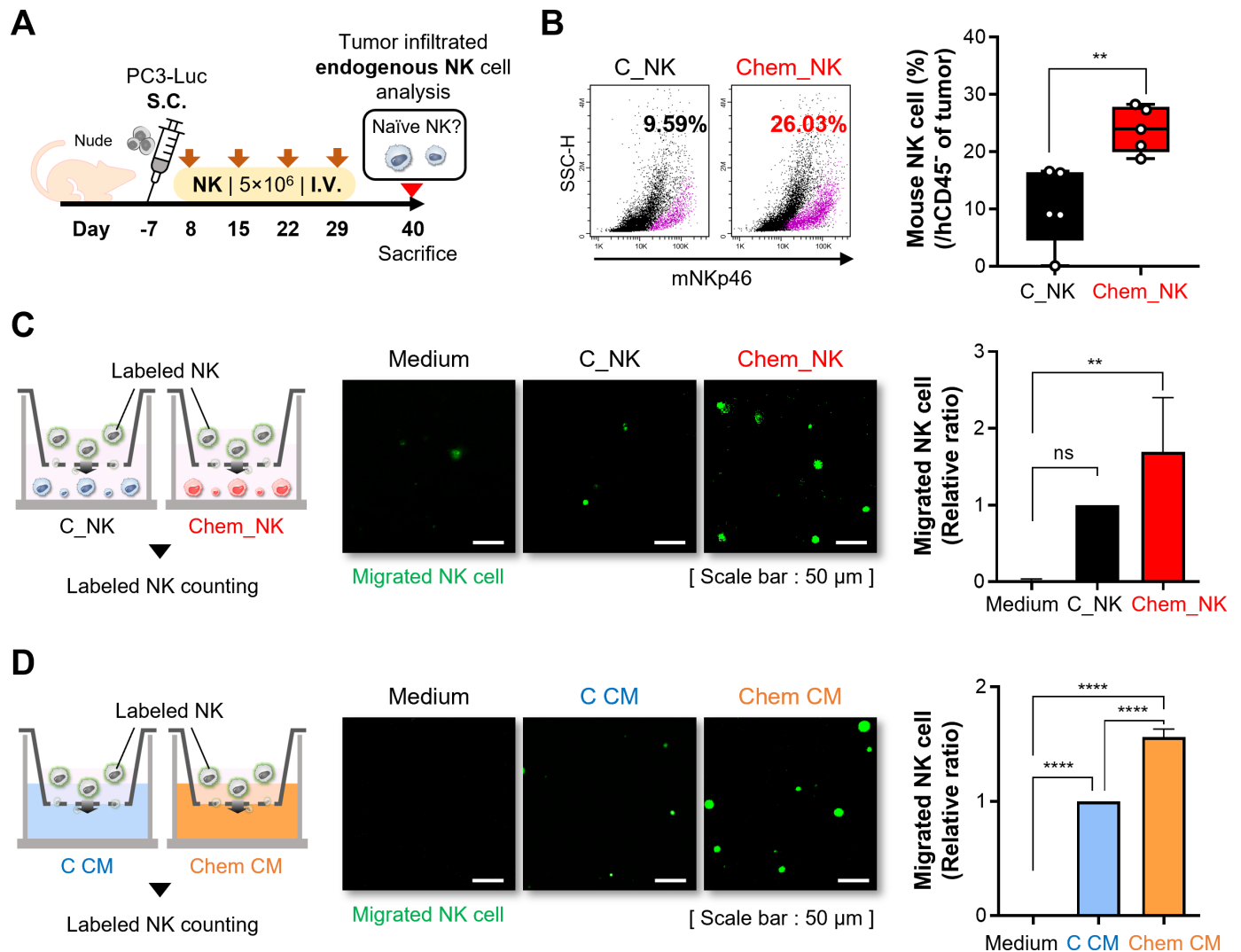
Figure 1 Chem_NK recruits other NK cells. (A) Schematic illustration of the PC-3 xenograft mouse model used to study the in vivo trafficking of mouse endogenous NK cells (each group n=5). Each type of NK-92MI cells was delivered intravenously to the tail. (B) Plots displaying the amount of mouse endogenous NK cells infiltrating the tumor. Statistical significance was evaluated using Student's t-test. For box and whisker plots, the horizontal line marks the median, the edges of the box represent the 25th and 75th percentile, and the whiskers show minimum and maximum values. (C) Schematic illustration of the transwell assay to evaluate migration of labeled NK-92MI cells toward C_NK or Chem_NK (left). Representative fluorescence microscopy images (middle) and a plot (right) displaying the relative ratio of migrated NK cells normalized to the C_NK group. Scale bar, 50 μm. (D) Schematic illustration of the transwell assay to evaluate migration of labeled NK-92MI cells toward C CM or Chem CM (left). Representative fluorescence microscopy images (middle) and a plot (right) displaying the relative ratio of migrated NK cells normalized to the C CM group. Scale bar, 50 μm. Each experiment was conducted at least three times. Data are presented as the mean±SD. Statistical significance was evaluated using an unpaired two-tailed t-test in B and one-way analysis of variance with Tukey's multiple comparison test in C–D. ns, not significant. **p<0.01 and ****p<0.0001. S.C., subcutaneous; I.V., intravenous; NK, natural killer; CM, conditioned media.

To evaluate whether CM enhances the tumor infiltration ability of adoptively transferred NK cells, we administered CM and NK-92MI cells in a nude mouse EO771 orthotopic model. When tumor volumes reached 500–700 mm³, CM (via intraperitoneally) and Carboxyfluorescein diacetate succinimidyl ester (CFSE)-labeled NK cells (via intravenously) were administered simultaneously, twice (figure 2G). Subsequently, the number of tumor-infiltrating NK cells was quantified (online supplemental figure 2). The Chem CM group exhibited significantly enhanced NK cell infiltration compared with

both the C CM and DPBS groups (figure 2H). These findings demonstrate that Chem CM treatment markedly increases NK cell infiltration into tumors, underscoring its potential to improve the efficacy of NK cell-based immunotherapies.

Chem CM enhances trafficking of NK cells to tumors by increasing their chemokine receptor expression

We next evaluated whether Chem CM enhances the cytotoxicity of NK cells in vitro. Unexpectedly, neither C CM nor Chem CM affected the cytotoxicity of NK
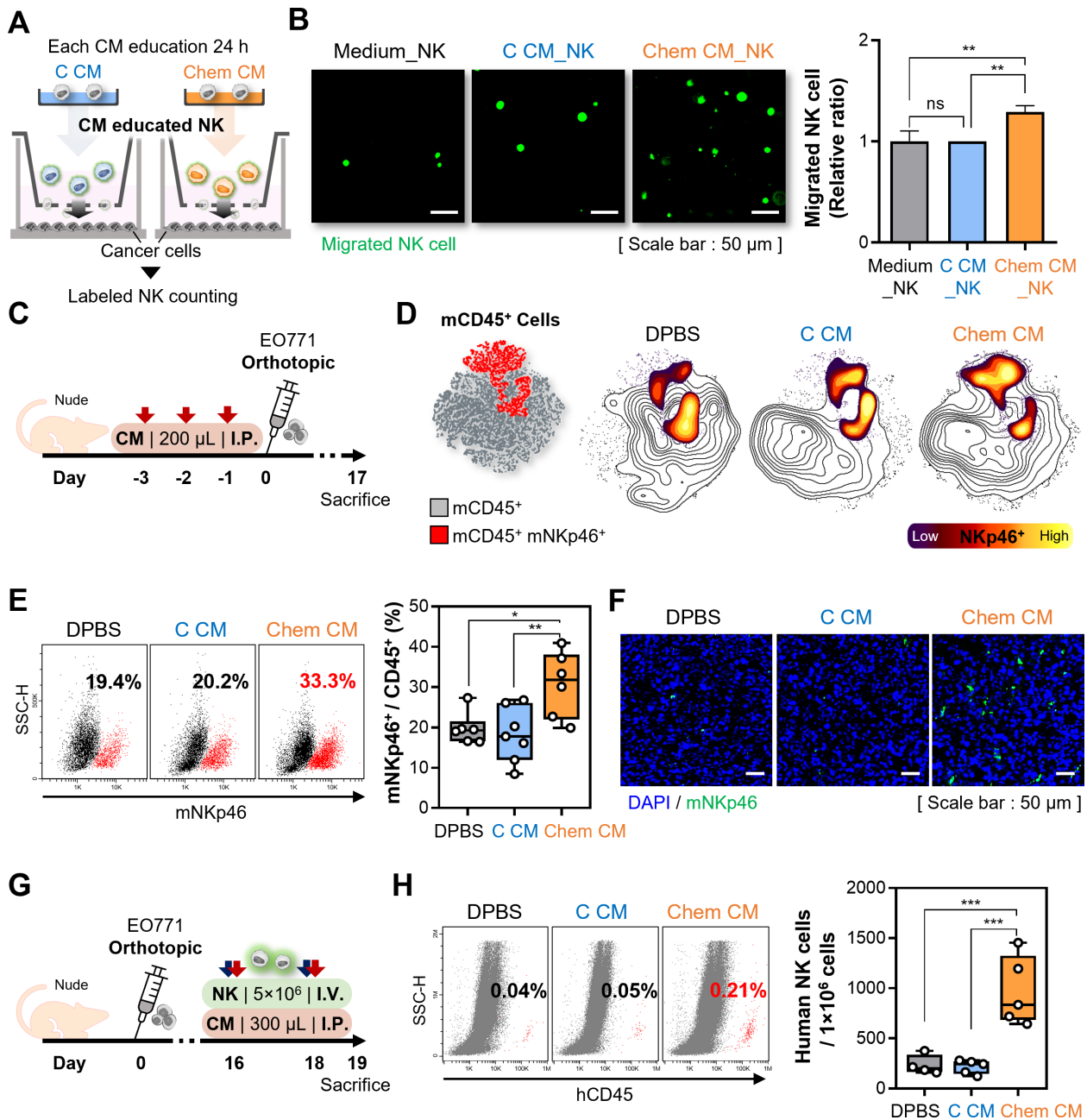
Figure 2 Chem CM promotes the migration of endogenous NK cells toward tumors. (A) Schematic illustration of the transwell assay to evaluate migration of C CM_NK or Chem CM_NK toward MDA-MB-231 cells. (B) Representative fluorescence microscopy images (left) and a plot (right) displaying the relative ratio of migrated NK cells normalized to the C CM_NK group. Scale bar, 50 μm. (C) Schematic of the EO771 orthotopic mouse model used to study the in vivo trafficking of endogenous NK cells (each group n=6~7). Each type of CM was injected intraperitoneally before tumor implantation. (D) Tumors were harvested 17 days after implantation, and the amount of endogenous NK cells infiltrating the tumor was visualized by t-SNE-CUDA and FlowSOM analyses. A FlowSOM plot (left) to display each cell population and a t-SNE plot (right) to compare the indicated sample groups. The uncolored contour plot represents CD45$^+$ cells, and the overlaid contour plot colored by density represents NKp46$^+$ cells. (E) The percentage of NK cells infiltrating the tumor was analyzed by flow cytometry and quantified in a graph. For box and whisker plots, the horizontal line marks the median, the edges of the box represent the 25th and 75th percentile, and the whiskers show minimum and maximum values. (F) Immunofluorescence staining of NK cells (green) with an anti-mNKp46 antibody and staining of nuclei (blue) with DAPI in the indicated tumor sections. Scale bar, 50 μm. Each experiment was conducted at least three times. (G) Schematic of the EO771 orthotopic mouse model used to study the in vivo trafficking of adoptively transferred NK cells, which are affected by Chem CM (each group n=4~5). (I) The number of human NK cells infiltrating the tumor was analyzed by flow cytometry and quantified per 1×10^6 tumor cells. Data are presented as the mean±SD. The statistical significance was determined by one-way analysis of variance with Tukey's multiple comparison test. *p<0.05, **p<0.01 and ***p<0.001. NK, natural killer; CM, conditioned media; I.P., intraperitoneal; I.V., intravenous; DPBS, dulbecco's phosphate-buffered saline; t-SNE-CUDA, t-distributed stochastic neighbor embedding compute unified device architecture.

cells (online supplemental figure 3). To investigate whether the enhanced migration ability of NK cells educated by CM contributes to cancer cell elimination, we performed real-time imaging of cleaved caspase-3/7 staining in cancer cells. This allowed us to quantify how quickly CM-educated NK cells eradicated target cells (figure 3A). Compared with C CM_NK, Chem CM_NK tracked to target cells more rapidly and induced higher levels of cleaved caspase-3/7 expression in cancer cells (figure 3B–E, online supplemental figure 4).

Immune cells migrate toward tumors by recognizing chemokines secreted by the target.[16 26 27] Specifically, they acquire homing abilities by sensing tumor-secreted chemokines with receptors such as CCR2, CCR4, CCR7, CX3CR1, CXCR3, CXCR4, and CXCR6 (figure 3F).[28–35] Therefore, we examined the expression levels of corresponding chemokine receptors in NK-92MI cells that were educated with C CM or Chem CM. Flow cytometric analysis revealed that hCCR4, hCCR7, hCXCR3, and hCXCR4 expressions were increased in Chem CM_NK (figure 3G, online supplemental figure 5). hCCR4 expression increased at the transcriptional level, while hCCR7, hCXCR3, and hCXCR4 expression increased without transcriptional activation, indicating Chem CM influences NK cells at both levels (online supplemental figure 6). Collectively, we concluded that Chem CM can enhance the homing ability of NK cells by increasing chemokine receptor expression, enabling them to more efficiently mobilize toward cancer cells.

Chem CM enhances anti-metastatic immunity of endogenous NK cells

Given the association between NK cell tumor infiltration and prognosis in patients,[14] we examined Chem CM's efficacy in immunocompetent mice. We established a lung metastasis mouse model by intravenously injecting B16-F10 cells into C57BL/6J mice. Subsequently, we administered the indicated CM intraperitoneally three times per week for 2 weeks (figure 4A). Mice showed no significant weight loss during the experimental period, indicating no potential side effects from Chem CM administration (online supplemental figure 7). At 14 days post-tumor implantation, formation of metastatic nodules in lungs was significantly reduced in mice injected with Chem CM (figure 4B). These findings were further confirmed by histological analysis of the lungs (figure 4C). In the analysis of the immune cell profile using t-SNE in the lungs, the mCD45$^+$ mNK1.1$^+$ mNKp46$^+$ cell population was notably increased in mice injected with Chem CM compared with mice injected with DPBS or C CM (figure 4D,E). Further quantification using flow cytometry confirmed that the percentage of activated NK cells increased significantly to an average of 7.46% in the Chem CM group compared with 4.62% in the DPBS group and 4.92% in the C CM group (figure 4F, online supplemental figure 8). Likewise, immunofluorescence staining detected a notable amount of NK cells in the lungs of mice injected with Chem CM (figure 4G). We next investigated whether the improved

tumor infiltration of endogenous mouse NK cells by Chem CM was due to increased expression of chemokine receptors. Consistent with figure 3G, mouse NK cells that infiltrated tumors in vivo exhibited substantially increased expression of mCCR4, mCXCR3, and mCXCR4 in the Chem CM group (figure 4H). These results suggest that Chem CM enhances chemokine receptor expression in endogenous mouse NK cells, linking to their tumor-homing activity and anti-metastatic efficacy.

To confirm whether the anti-metastatic effect is mediated by endogenous NK cells, we conducted NK cell depletion studies in C57BL/6J mice. For NK cell depletion, anti-Asialo GM1 antibody was administered 1 day before cancer cell injection. The following day, mice were injected intravenously with B16-F10 cells (1×10^6 cells). As shown in online supplemental figure 9A, the CM and anti-Asialo GM1 antibody were administered intraperitoneally thrice weekly and every 3 days, respectively. After 2 weeks of observation, we confirmed that the Chem CM treatment group significantly suppressed lung metastasis compared with the DPBS group; however, this effect was diminished by anti-Asialo GM1 (online supplemental figure 9B). These results suggest that Chem CM enhances the tumor-homing activity of endogenous NK cells, thereby inducing anti-metastatic efficacy.

Chem_NK extensively secrete a diverse array of cytokines
We quantified the protein content in each CM and found that Chem_NK secreted more protein than C_NK (figure 5A). To evaluate the biological role of proteins present in CM, we treated CM with proteinase K to degrade the secreted proteins and analyzed the ability of NK cells to migrate toward cancer cells. The addition of proteinase K to Chem CM reduced its ability to enhance the migration of NK cells, indicating that proteins in CM are critical to boost the migration capacity of NK cells (figure 5B). Subsequently, a cytokine array was conducted to identify the upregulated proteins. Notably, out of 105 cytokines tested, 28 cytokines including IFN-γ were upregulated in Chem CM compared with C CM (figure 5C,D). To assess the biological activities of the upregulated cytokines in Chem CM, we conducted Gene Ontology (GO) analysis of 28 cytokines. This analysis indicated that these cytokines were associated with the activities of several signaling pathways, including the ERK and JAK/STAT signaling pathways (figure 5E). These results suggest that Chem CM enhances migration of NK cells by activating the ERK and/or JAK/STAT signaling pathways.

The effect of Chem CM on the migration of recipient NK cells depends on the ERK1/2 pathway
JAK/STAT signaling is primarily activated by IFN-γ, recruiting NK cells to target cancer cells.[33] To investigate the involvement of JAK/STAT signaling in enhanced migration of NK cells on exposure to Chem CM, we initially examined the impact of Chem CM on JAK/STAT signaling activity (online supplemental figure 10A). Unexpectedly, the activity of JAK/STAT signaling, represented
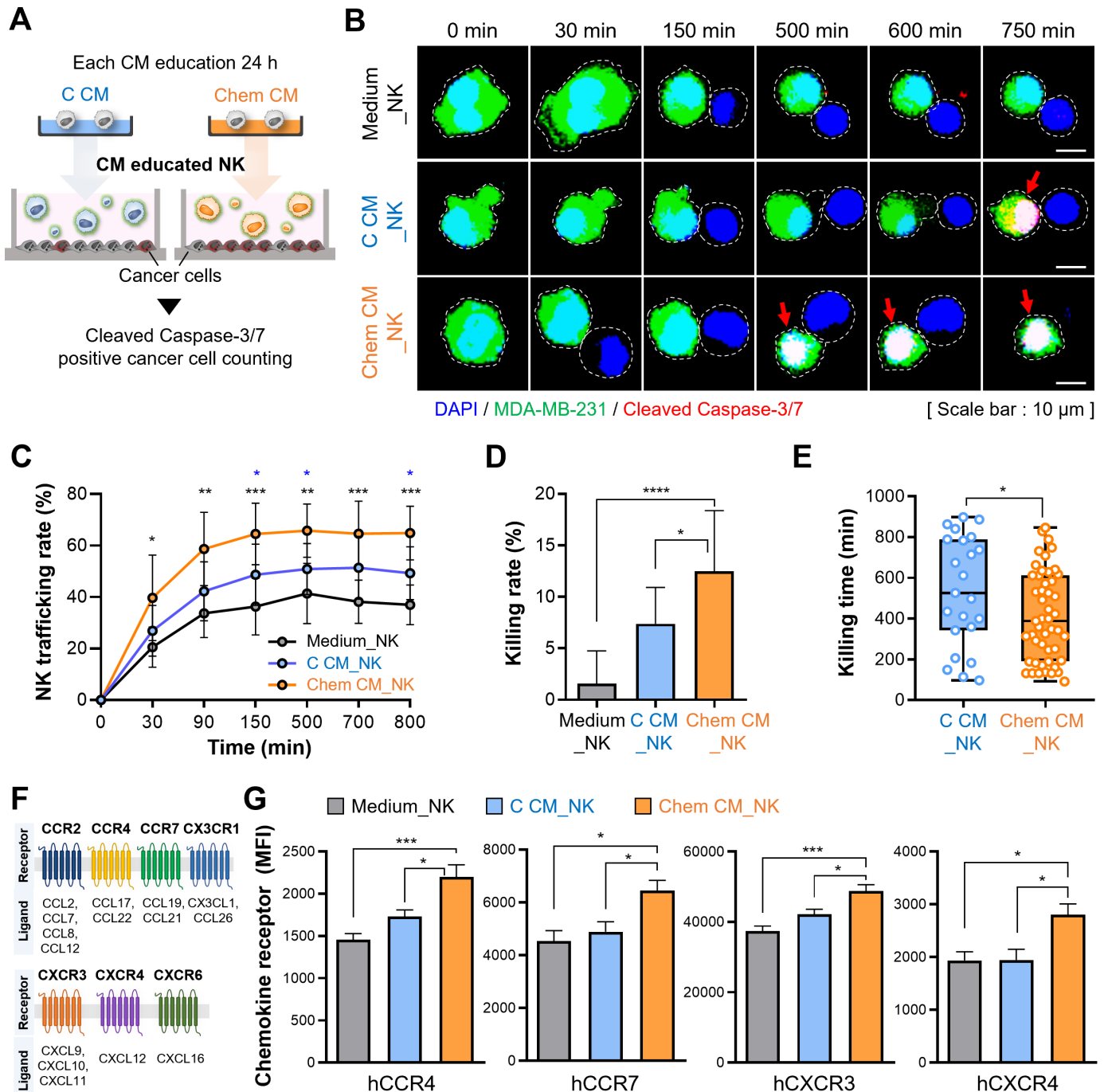
Figure 3 Chem CM enhances the trafficking activity of NK cells toward tumors by upregulating expression of chemokine receptors. (A) Schematic illustration of the cleaved caspase-3/7 assay to evaluate the ability of C CM_NK or Chem CM_NK to eradicate MDA-MB-231 cells. (B) Representative real-time images of cleaved caspase-3/7 (red) in MDA-MB-231 cells (green) during co-culture with NK-92MI cells treated with each CM. Nuclei were stained with DAPI (blue). Arrows indicate cleaved caspase-3/7-positive targets. Scale bar, 10 µm. (C) The percentage of NK cells trafficking to the target at the indicated time points (n=209 for medium, n=232 for C CM_NK, and n=186 for Chem CM_NK). (D) The ratio of cleaved caspase-3/7-positive target cells after stable contact with NK cells under the indicated conditions. (E) The time required for individual NK cells to kill a single target cell (killing time). Each data point represents the time taken by one NK cell to eliminate a target cell (n=23 for C CM_NK and n=49 for Chem CM_NK). For box and whisker plots, the horizontal line marks the median, the edges of the box represent the 25th and 75th percentile, and the whiskers show minimum and maximum values. (F) Chemokine receptors of NK-92MI cells and their ligands. (G) Expression of the indicated chemokine receptors in C CM_NK and Chem CM_NK was analyzed by flow cytometry and expressed as mean fluorescence intensity (MFI). Each experiment was conducted at least three times. Data are presented as the mean±SD. Statistical significance was evaluated using two-way analysis of variance with Tukey's multiple comparison test in G, one-way analysis of variance with Tukey's multiple comparison test in D and G, and an unpaired two-tailed t-test in E. ns, not significant. *p<0.05, **p<0.01, and ***p<0.001. NK, natural killer; CM, conditioned media; DAPI, 4',6-diamidino-2-phenylindole.
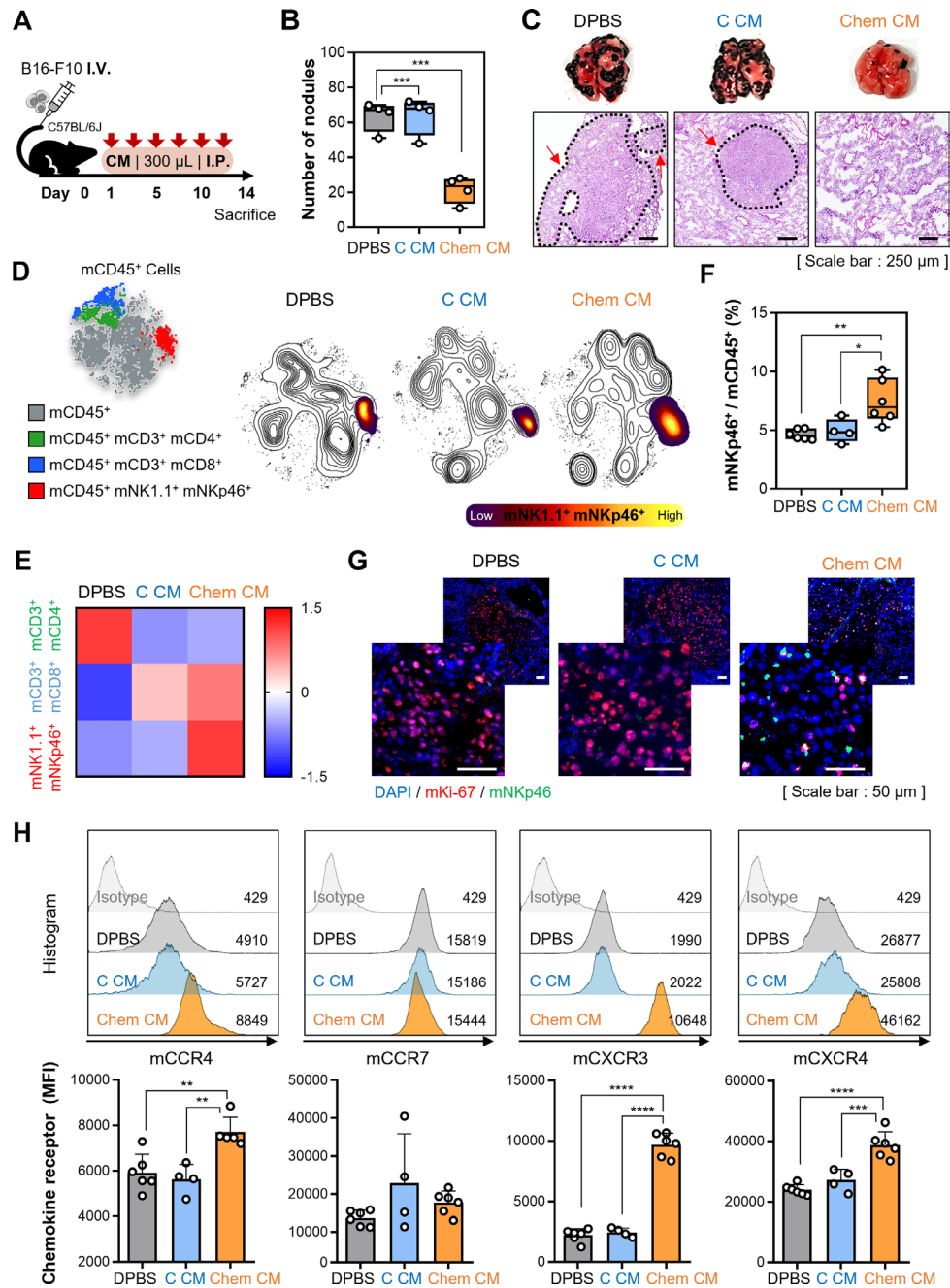
Figure 4 Chem CM exhibits anti-metastatic immunity by increasing tumor infiltration of endogenous NK cells. (A) Schematic of the B16-F10 lung metastasis mouse model used to study the in vivo antitumor efficacy of endogenous NK cells (each group n=4~6). (B) Lungs were harvested 14 days after tumor implantation, and the number of lung metastatic nodules was counted. (C) Representative H&E staining of sections from mouse lungs. Arrows indicate metastatic foci. Scale bar, 250 μm. (D) Visualization of the amount of endogenous NK cells in lungs by t-SNE-CUDA and FlowSOM analyses. A FlowSOM plot (left) to display each cell population and a density plot of t-SNE plots (right) to compare the indicated sample groups. The uncolored contour plot represents mCD45$^+$ cells, and the overlaid contour plot colored by density represents mNK1.1$^+$ mNKp46$^+$ cells. (E) Heatmap showing the percentage of NK and T cells in the lungs in each group determined by t-SNE analysis. The scale bar is a Z-score computed across cell types for each population. (F) The percentage of intratumoral mNKp46$^+$ cells among mCD45$^+$ cells was analyzed by flow cytometry and quantified in a graph. (G) Immunofluorescence staining of NK cells (green) with an anti-mNKp46 antibody, tumor cells (red) with an anti-mKi-67 antibody, and nuclei (blue) with DAPI in the indicated tumor-bearing lung sections. Scale bar, 50 μm. (H) Expression of the indicated chemokine receptors in mNKp46$^+$ cells within each group was quantified by flow cytometry. For box and whisker plots, the horizontal line marks the median, the edges of the box represent the 25th and 75th percentile, and the whiskers show minimum and maximum values. Data are presented as the mean±SD. Statistical significance was evaluated using one-way analysis of variance with Tukey's multiple comparison test. *p<0.05, **p<0.01, ***p<0.001, and ****p<0.0001. NK, natural killer; CM, conditioned media; I.P., intraperitoneal; I.V., intravenous; MFI, mean fluorescence intensity; DPBS, dulbecco's phosphate-buffered saline; t-SNE-CUDA, t-distributed stochastic neighbor embedding compute unified device architecture; DAPI, 4',6-diamidino-2-phenylindole.
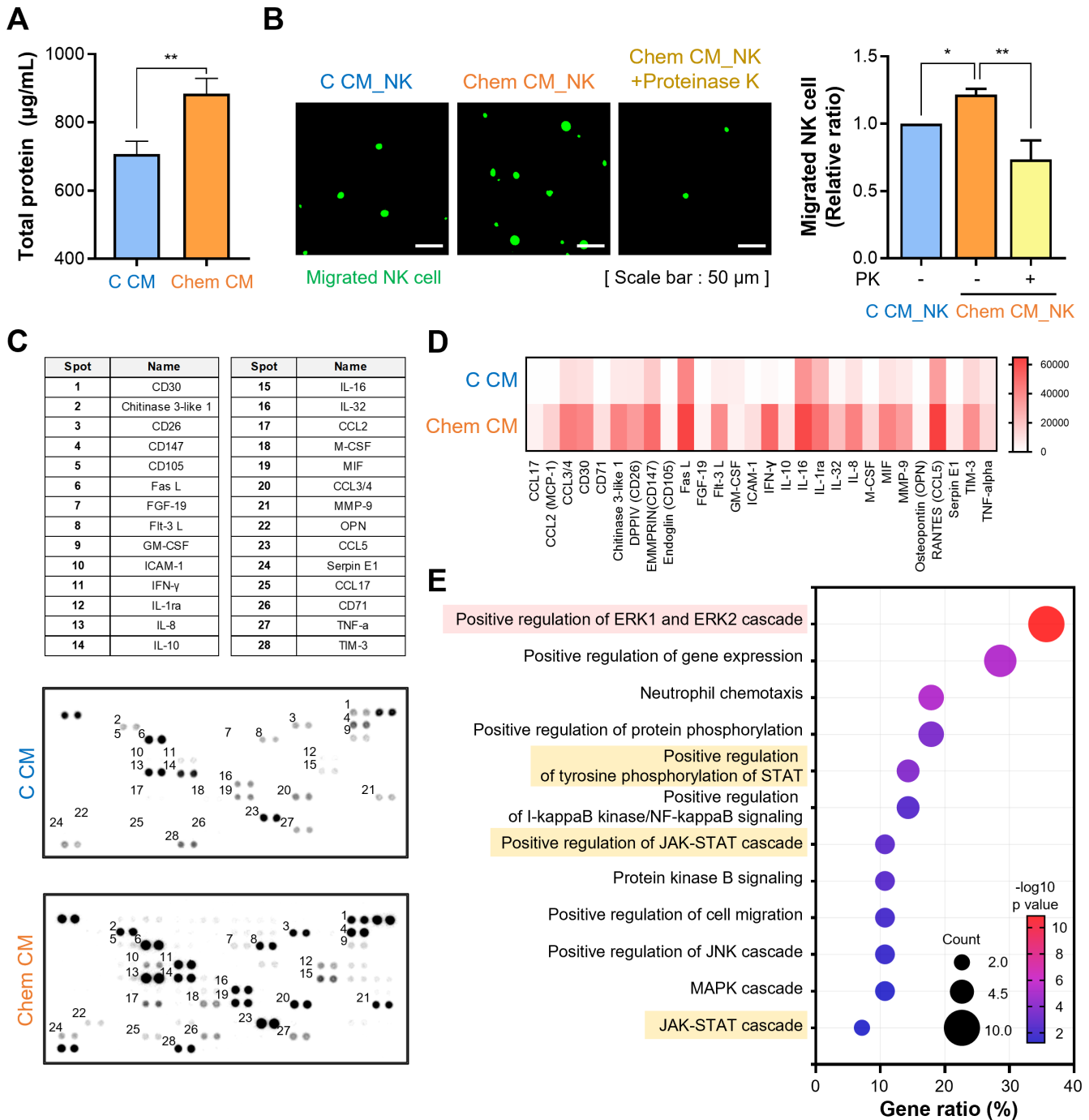
Figure 5 Chem_NK extensively secrete a diverse array of cytokines. (A) The total protein concentration in each CM was measured by the BCA assay. Statistical significance was evaluated using Student's t-test. (B) NK-92MI cells were incubated in Chem CM with or without proteinase K (PK, 0.2 µg/mL) for 24 hours. Representative fluorescence microscopy images (left) and a plot (right) displaying the relative ratio of migrated NK cells normalized to the C CM_NK group. Scale bar, 50 µm. The experiment was conducted at least three times. Statistical significance was evaluated using one-way analysis of variance with Tukey's multiple comparison test. **p<0.01. (C) Analysis of cytokine profiles within 500 µL of each CM using a Proteome Profiler Human XL Cytokine Array Kit. Antibodies to detect each cytokine are represented by duplicate spots, and the locations of the spotted antibodies are presented in the table. (D) Heatmap analysis was performed to display the cytokine signal measurements corresponding to the data presented in C and to compare differences between each CM. The density of an individual dot reflects the signal intensity of the cytokine, which was measured using ImageJ. The scale bar is a measurement determined based on the pixel density. (E) A dot plot showing the top enriched Gene Ontology biological processes of Chem CM determined from significant differentially expressed genes. The size of the circle represents gene number, the color represents −log10 of the p value, and enrichment terms were ranked by gene number. Functional enrichment analysis was performed using DAVID software. Data are presented as the mean±SD. Statistical significance was evaluated using an unpaired two-tailed t-test in A and one-way ANOVA with Tukey's multiple comparison test in B. *p<0.05, and **p<0.01. NK, natural killer; CM, conditioned media; BCA, bicinchoninic Acid; GO, gene ontology.

by STAT1 phosphorylation, was unaffected by Chem CM treatment (online supplemental figure 10B,C). In line with this, blockade of the IFN-γ receptor in NK cells with antibodies during incubation with Chem CM did not alter the enhanced mobility of NK cells (online supplemental figure 10D). This suggests that other factors present in Chem CM apart from IFN-γ exert effects.

Given that ERK signaling is also reported to play a crucial role in NK cell migration (figure 6A),[36–38] we investigated whether it is activated by Chem CM in NK cells. NK cells incubated in Chem CM exhibited increased ERK phosphorylation (figure 6B). To confirm the significance of this pathway in NK cells educated by Chem CM, we chemically inhibited ERK signaling in NK cells during their incubation with Chem CM and examined their migration ability toward cancer cells. The ERK inhibitor U0126 impaired NK cells from being educated by Chem CM to exhibit enhanced migration toward cancer cells (figure 6C). Furthermore, the enhanced expression of chemokine receptors in NK cells exposed to Chem CM was hindered by chemical inhibition of ERK signaling (figure 6D).

Finally, we investigated whether the upregulation of chemokine receptors induced by ERK signaling was due to cytokines upregulated in Chem CM. To explore this, we performed protein-protein interaction analysis using the search tool for the retrieval of interacting genes/proteins (STRING) database, which identified seven candidate cytokines associated with ERK signaling (online supplemental figure 11). Additionally, DAVID analysis highlighted 11 cytokines with high relevance to the "Positive regulation of ERK1 and ERK2 cascade" pathway. From these, we selected ICAM-1, TNF-α, CCL3, CCL4, CCL5, and CCL17 as key candidates involved in increasing ERK phosphorylation[36–41] (figure 6E). When NK cells were incubated in C CM containing a mixture of these selected cytokines, expression of chemokine receptors significantly increased (figure 6F). Collectively, these results suggest that the array of cytokines in Chem CM enhances migration of NK cells toward cancer cells by activating ERK signaling and increasing chemokine receptor expression.

DISCUSSION AND CONCLUSION
NK cell-based immunotherapy, particularly with CAR-NK cells, has demonstrated both safety and efficacy against CD19-positive lymphoid tumors.[7 8] The potential to generate allogeneic "off-the-shelf"" products enhances the prospects of NK cells as a compelling candidate for anticancer immune cell therapy. To broaden NK cell therapy for solid tumors, understanding NK cell homing and trafficking mechanisms is essential. This will provide additional strategies to boost the infiltration and anti-tumor immune responses of both endogenous NK cells and adoptively transferred ones. Currently, several strategies, including genetic engineering, are being developed to improve NK cell migration and tumor homing.[16 42–44]

Given that NK cells produce diverse cytokines based on stimuli,[45] using NK cell secretomes, generated through optimal priming, to educate neighboring NK cells and enhance their mobility or tumor-homing ability is a promising approach. According to our data, a myriad of molecules, including IFN-γ, are prominently secreted by NK cells chemically primed with 25KbPEI. These secretomes can direct recipient NK cells, resulting in enhanced migration abilities toward cancer cells in vitro and improved tumor infiltration abilities of endogenous NK cells in vivo. While IFN-γ is notably present in Chem CM compared with C CM, experiments in which the IFN-γ receptor was blocked indicate that other factors contribute more to the enhancement of NK cell migration. Given that the levels of numerous cytokines are increased in Chem CM, the educative impact of the secretomes on other NK cells may be mediated by a combination of several factors rather than by specific molecules.

We focused solely on evaluating the expression profiles of 105 cytokines associated with immune cell chemotaxis; therefore, the possibility that the activity of Chem CM was influenced by alternative secretomes, such as those of exosomes, cannot be ruled out. Recent evidence suggests that exosomes derived from immune cells, including NK cells, modulate immune responses and enhance antitumor activity by shaping the tumor microenvironment.[46–48] These exosomes contain typical NK cell components, including perforin and granzymes.[49 50] While there are no reports on the educational activity of NK cell-derived exosomes on other immune cells, further investigation is essential to determine whether the educational activity of Chem CM is mediated by exosomes. By performing GO analysis of highly secreted cytokines, we examined the impact of Chem CM on two signaling pathways in NK cells. Investigating the involvement of exosomes in the biological activity of Chem CM is anticipated to broaden the spectrum of candidate signaling pathways associated with the enhanced migration of NK cells.

Our data demonstrate that Chem CM has the potential to enhance the expression of chemokine receptors in NK cells at both the transcriptional and translational levels. Specifically, CCR4 expression was upregulated transcriptionally, whereas CCR7, CXCR3, and CXCR4 showed increased expression without transcriptional changes. Since we identified ERK signaling as an upstream regulator of the chemokine receptor expression, it is plausible that activation of ERK signaling simultaneously triggers both transcriptional and translational machinery.

The increased presence of NK cells with enhanced chemokine receptor expression in the lungs of Chem CM-injected mice, compared with those injected with C CM, suggests that the anti-metastatic efficacy of Chem CM is primarily due to its ability to educate endogenous NK cells. This conclusion is further supported by the diminished antitumor activity of Chem CM in immune-competent mice following the depletion of endogenous NK cells, underscoring NK cells as the primary targets of
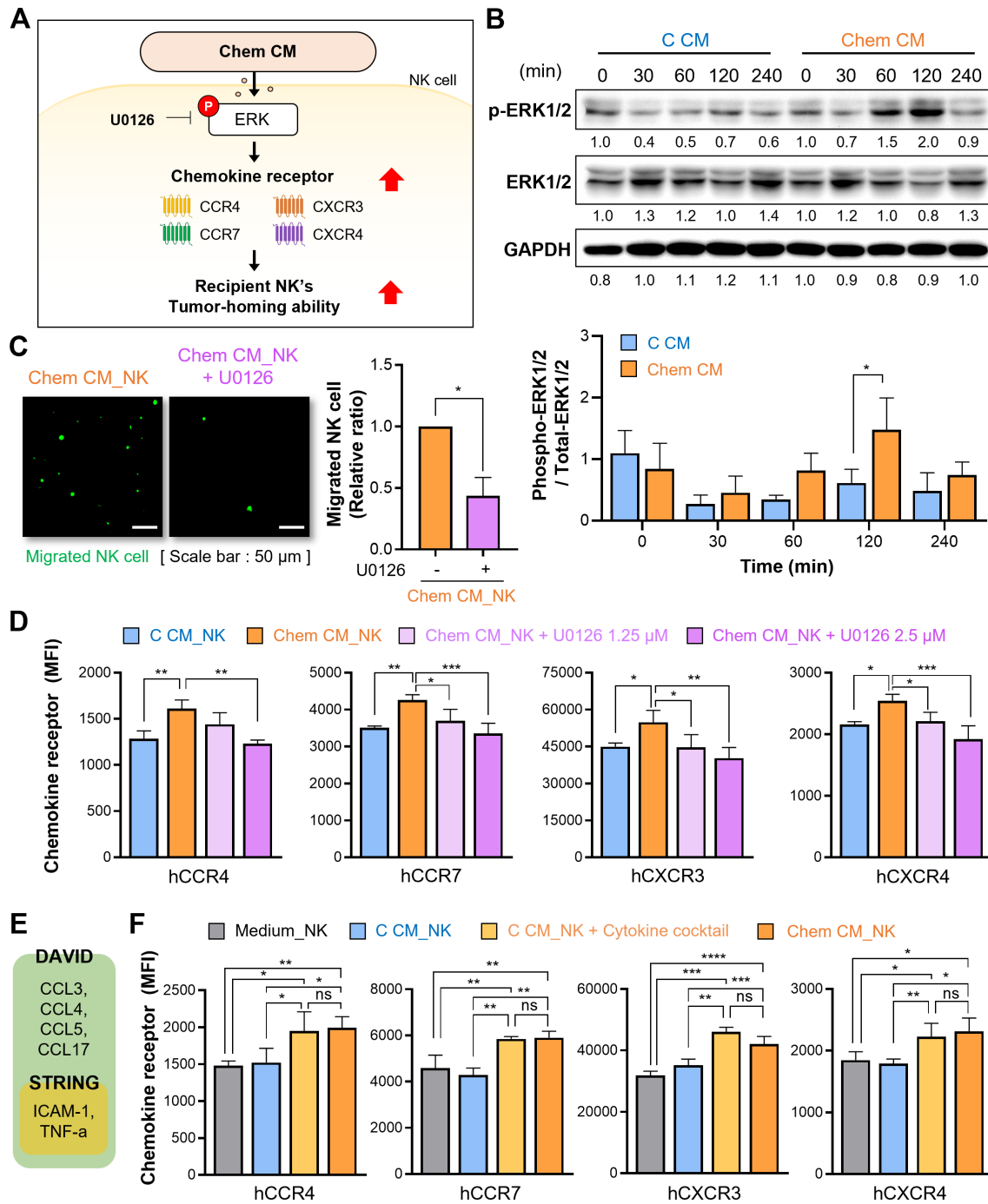
Figure 6 The effect of Chem CM on migration of recipient NK cells depends on the ERK1/2 pathway. (A) Hypothesis regarding the ERK signaling pathway in Chem CM_NK. Chem CM enhances the tumor homing ability of recipient NK cells by increasing their chemokine receptors. (B) Immunoblotting was performed to detect ERK phosphorylation in NK-92MI cells treated with each CM for the indicated durations (top). The band intensities were quantified using ImageJ, and the ratio of p-ERK1/2 to total ERK1/2 is presented in the graph (bottom). Statistical analysis was conducted using a two-way ANOVA with Sidak's multiple comparisons test (vs C CM). (C) NK-92MI cells were incubated in Chem CM with or without U0126 (10 μM) for 24 hours. Representative fluorescence microscopy images (left) and a plot (right) displaying the relative ratio of migrated NK cells normalized to the Chem CM_NK without U0126 group. Statistical significance was evaluated using the Student's t-test. Scale bar, 100 μm. (D) NK-92MI cells were incubated in Chem CM with or without U0126 (1.25 or 2.5 μM) for 12 hours, and then expression of the indicated chemokine receptors was determined by flow cytometry and expressed as MFI. (E) Candidate cytokines involved in the effect of Chem CM. (F) NK-92MI cells were incubated in culture medium, C CM, C CM with the indicated cytokines or Chem CM for 24 hours, and then expression of chemokine receptors was analyzed by flow cytometry and expressed as MFI. Data are presented as the mean±SD. Statistical significance was evaluated using two-way analysis of variance with Sidak's multiple comparison test in B, a paired two-tailed t-test in C, and one-way analysis of variance with Tukey's multiple comparison test in D and F. ns, not significant. *p<0.05, **p<0.01, ***p<0.001, and ****p<0.0001. NK, natural killer; CM, conditioned media; MFI, mean fluorescence intensity.

Chem_NK in exerting its antitumor effects. Nevertheless, the possibility that other immune cells are also influenced by Chem CM cannot be excluded. Preliminary data indicate a decrease in regulatory T cells, a slight increase in M2 macrophages, and a reduction in M1 macrophages in the metastatic lungs of Chem CM-injected mice (data not shown). These observations suggest that Chem CM may influence the composition of immune cell populations in the tumor microenvironment. Further investigations are needed to determine the functional implications of these immune alterations, including their potential role in metastatic progression.

Additionally, despite donor variation, our preliminary experiments reveal that human primary NK cells purified from the peripheral blood mononuclear cells of healthy donors respond to Chem CM. This response includes enhanced migration toward cancer cells and increased chemokine receptor expression. These observations imply that the Chem_NK's effects are not limited to the NK-92MI cell line or mouse NK cells, broadening its potential applicability in antitumor therapeutics. Therefore, Chem CM represents a promising candidate for therapeutic cancer vaccines or adjuvants, with its adaptability to various vaccine platforms and immune adjuvants underscoring its potential to advance cancer immunotherapy.

One notable application of Chem CM is its ability to enhance the tumor homing activity of adoptively transferred therapeutic NK cells. As demonstrated in figure 2G–H, co-administration of Chem CM with NK cells significantly improves tumor infiltration of the transferred cells. Given that tumor homing is critical for NK cell-mediated antitumor efficacy, Chem CM has the potential to serve as a supplement to optimize NK cell-based therapies for solid tumors. Additionally, body weight monitoring throughout the experimental period revealed no detectable changes in mice treated with Chem CM, supporting the potential safety for clinical application (online supplemental figure 7).

Finally, Chem CM may contain a diverse array of immune-active molecules beyond cytokines, offering valuable insights for designing next-generation therapeutic cancer vaccines or adjuvants.

In summary, we suggest that Chem CM is a promising candidate for the development of therapeutic cancer vaccines or adjuvants. Its versatility in tailoring vaccine platforms and immune adjuvants further underscores its potential in advancing cancer immunotherapy.

MATERIALS AND METHODS
Materials
A stock solution of 25KbPEI (408727; Sigma-Aldrich, Missouri, USA) was diluted to a concentration of 5 mg/mL using ultrapure distilled water.[23] Proteinase K (p6556; Sigma-Aldrich) was added during the CM production process at the indicated concentrations. The JAK2 inhibitor WP1130 (681685; Sigma-Aldrich), the IFN-γ receptor blocker IFN-γR antibody (MAB6731; R&D Systems, Minnesota, USA), and the ERK inhibitor U0126 (9903S; Cell Signaling Technology, Massachusetts, USA) were added to NK-92MI cells at the indicated concentrations before or during CM treatment. Recombinant human ICAM-1 (150-05), CCL3 (300-08), CCL4 (300-09), CCL5 (300-06), CCL17 (300-30), and TNF-α (300–01A) were purchased from PeproTech (New Jersey, USA).

Cell culture
The human NK cell line NK-92MI was maintained in Alpha Minimum Essential Medium (12561056; Gibco/Life Technologies, New York, USA) supplemented with 2 mM L-glutamine (GIB-25 030–81; Gibco/Life Technologies), 0.1 mM 2-mercaptoethanol (21985–023; Gibco/Life Technologies), 0.02 mM folic acid (F8758; Sigma-Aldrich), 0.2 mM myo-inositol (I7508; Sigma-Aldrich), 1% penicillin/streptomycin (15140122; Gibco/Life Technologies), and 12.5% fetal bovine serum (FBS, TFS-12483020; Gibco/Life Technologies). The human breast cancer cell line MDA-MB-231, the murine breast cancer cell line EO771, and the melanoma cancer cell line B16-F10 were cultured in Dulbecco's Modified Eagle Medium (11995073; DMEM, Gibco/Life Technologies) supplemented with 10% FBS and 1% penicillin/streptomycin. All cells were purchased from the American Type Culture Collection (Virginia, USA), and cultured at 37°C in a 5% CO_2 incubator.

Preparation of CM
Chem_NK were generated by treating 5×10^5 cells/mL NK-92MI cells with 5 µg/mL 25KbPEI for 12 hours as previously reported.[23] To prepare C CM and Chem CM, NK cells were seeded at a density of 5×10^5 cells/mL and incubated for 24 hours in serum-free and phenol-free medium. Then, the supernatant was collected by centrifugation, and cellular debris was eliminated using 0.22 µm syringe filters (SLGPR33RS; Millipore, Massachusetts, USA). The CM was concentrated by 10-fold using 3K MWCO Pierce Protein Concentrators PES (88526; Thermo Fisher Scientific, Massachusetts, USA), following the manufacturer's instructions.

Migration assay
The migration ability of NK cells was investigated using a 24-well insert Transwell chamber (8.0 µm, 353097; Corning, New Jersey, USA). To confirm the migration ability toward cancer cells, MDA-MB-231 cells (5×10^5) were seeded into the bottom chamber in serum-free medium and incubated for 12 hours. NK cells (5×10^5) were labeled with 1 µM CellTrace CFSE (C34554; Thermo Fisher Scientific) and loaded into the upper chamber in serum-free medium. After 18 hours, CFSE-stained NK cells in the lower chamber were counted using a Luna cell counter (Logus biosystems, Gyeonggi-do, Republic of Korea). An EVOS M5000 imaging system (Invitrogen, Massachusetts, USA) was used for imaging.

Live cell imaging of confocal microscopy

MDA-MB-231 cells (target) were pre-stained with a Cell-Trace Far Red Cell Proliferation Kit (C34564; Invitrogen). Then, 3×10^3 labeled MDA-MB-231 cells were seeded in a confocal plate and co-cultured with 3×10^3 NK cells in DMEM containing 5% FBS. Binding between NK and MDA-MB-231 cells was evaluated by tracking the movement of individual NK cells with a time-lapse microscope. Once stable binding ($\geq$10 min) was established, the time required for NK cells to lyse cancer cells was recorded for each field of view. The overall killing efficiency was determined by dividing the number of apoptotic target cells by the total number of target cells. A modified Olympus FV3000 microscope (Olympus, Hachioji, Tokyo) equipped with a 20×objective lens (UPlanXApo, numerical aperture=0.8). The imaging conditions were sustained using an Olympus FV3000 incubation system (INCUBATOR T; Live Cell Instruments, Seoul, Republic of Korea). Imaging data were analyzed with Olympus cellSens software.

In vivo animal experiments

Evaluation of intratumoral infiltration of endogenous NK cells: To investigate the activity of Chem CM, the tumor cell samples from the study published in Choi *et al* were used.[51] The tumor cell samples were obtained from an established PC-3-Luc cell xenograft model in male BALB/c nude mice (6 weeks). At 7 days after cancer cell injection, DPBS or each type of 5×10^6 NK cells were intravenously injected once a week for 4 weeks. At 39 days, the tumors were dissociated into single cells and stained with an FITC-mNKp46 antibody (137606; BioLegend, California, USA), and PE-hCD45 antibody (564253; BD Biosciences, New Jersey, USA) to analyze the population of endogenous NK cells infiltrating into the tumor.

Evaluation of the effect of CM on intratumoral infiltration of NK cells: female BALB/c nude mice (5 weeks) were injected with DPBS or each type of CM intraperitoneally daily for 3 days. After 1 day, 2×10^5 EO771 cells were suspended in 100 µL of a mixture of phosphate-buffered saline (PBS) and Matrigel (BD Biosciences) at a 1:1 ratio and injected into the fourth mammary fat pads of each mouse. When the tumor volume reached 700 mm^3, endogenous NK cells in the tumor were analyzed by FITC-mNKp46 antibody. 2×10^5 EO771 cells were injected into the fourth mammary fat pad of each female BALB/c nude mice under the conditions described above. When the tumor volume reached 500–700 mm^3, CM was injected intraperitoneally and 5×10^6 NK-92MI cells were injected intravenously twice. The next day, adoptively transferred NK cells in the tumor were analyzed by PE-hCD45 antibody (304058; BioLegend).

Evaluation of the antitumor effect of CM on endogenous NK cells: female C57BL/6J mice (5 weeks) were injected with 1×10^6 B16-F10 melanoma cells suspended in 100 µL of PBS into the tail vein. The next day, DPBS or each type of CM (300 µL) started to be intraperitoneally injected three times per week for 12 days. At 14 days after injection of melanoma cells, the lungs were harvested for analysis. The immune cell population was analyzed using the following antibodies (all from BioLegend): PE/Cyanine7-mCD45 (103114), APC/Cyanine7-mNK1.1 (108724), APC-mNKp46 (137608), Brilliant Violet 421-mCD3 (100228), PerCP-mCD4 (100538), and Alexa Fluor 700-mCD8a (100730).

All mice were purchased from JA Bio (Gyeonggi-do, Republic of Korea).

Flow cytometric analysis

NK cells were stained with a Zombie Aqua Fixable Viability Kit (423102; BioLegend) for 15 min in the dark to distinguish live and dead cells, fixed with 1% paraformaldehyde for 15 min, and washed with stain buffer (DPBS containing 0.09% sodium azide and 2% FBS). Fixed cells were stained using an appropriate combination of antibodies for 30 min in flow cytometry buffer in the dark at room temperature and washed with stain buffer. Data was acquired using a CytoFLEX flow cytometer (Beckman Coulter, California, USA) and analyzed using CytExpert (Beckman Coulter) and Kaluza (Beckman Coulter). The following antibodies were used (all from BioLegend): PE-hCCR4 (359405), PerCP/Cyanine5.5-hCCR7 (353204), PE-hCXCR3 (353705), PerCP/Cyanine5.5-hCXCR4 (306515), APC-mCCR4 (131211), APC-mCCR7 (120107), APC-mCXCR3 (126511), and APC-mCXCR4 (146507).

Immunohistochemistry and immunofluorescence

Paraffin-embedded tumor blocks were sectioned at a thickness of 6 µm using a microtome (Leica, Hesse, Germany). Following blocking with Protein Block Serum-Free solution (X0909; Agilent, California, USA), sections were stained overnight at 4°C in the dark with FITC-mNKp46 antibody to observe the distribution of infiltrated NK cells in tumor. Nuclei were stained with DAPI (12333553; Invitrogen). Sections were imaged using a fluorescence microscope (Carl Zeiss, BW, Germany) and analyzed using ImageJ software (ImageJ, Maryland, USA).

OCT compound (4583; sakura, California, USA) embedded metastatic lung tissue blocks were sectioned at a thickness of 8 µm using a cryotome (Leica). To visualize lung metastatic nodules, sectioned lung tissues underwent H&E staining using Harris' hematoxylin solution (1.09253; Sigma-Aldrich) and Eosin Y solution (1.09844; Sigma-Aldrich). Stained lung tissue was imaged using an optical microscope (Nikon Corporation, Tokyo, Japan). To observe the distribution of infiltrated NK cells in the tumor, sections were permeabilized, blocked with Protein Block Serum-Free solution, and stained with FITC-mNKp46 and PE/Dazzle 594-anti-mouse mKi-67 (352428; BioLegend) antibodies overnight at 4°C. Nuclei were stained with DAPI, and slides were mounted using Fluorescence Mounting Medium. Sections were imaged using a fluorescence microscope and analyzed using ImageJ software.

Cytokine array

The cytokine profiles of CM of NK-92MI cells were analyzed using a Proteome Profiler Human XL Cytokine Array Kit (ARY022B; R&D Systems), which consists of 105 cytokine and chemokine antibodies spotted in duplicate onto a membrane. Analysis was conducted according to the manufacturer's protocol. Briefly, blots were blocked for 1 hour and incubated overnight at 4°C with 500 µL of each CM. Immuno-spots were quantified using ImageJ software. Protein–protein interaction analysis was performed using the STRING platform with Cytoscape software (V.3.10.2).[52]

Immunoblotting

Cells were harvested and lysed in cell lysis buffer (9803S; Cell Signaling Technology) containing a protease and phosphatase inhibitor cocktail (P3300-001; GenDEPOT, Texas, USA). Following separation by sodium dodecyl sulfate-polyacrylamide gel electrophoresis, cell lysates were transferred to a polyacrylamide difluoride membrane (1620177; Bio-Rad, California, USA). Membranes were blocked for 1 hour, incubated with appropriate primary antibodies overnight at 4°C, and then incubated with a secondary antibody at room temperature for 1 hour. Primary antibodies (all from Cell Signaling Technology) included phospho-Stat1 (Tyr701) (9167), p44/42 MAPK (Erk1/2) (4695), phospho-p44/42 MAPK (p-Erk1/2, Thr202/Tyr204) (4370), and GAPDH (3683). Secondary antibodies included Goat Anti-Rabbit IgG antibody (HRP) (GTX213110-01; GeneTex, California, USA), and Goat Anti-Mouse IgG antibody (HRP) (GTX213111-01; GeneTex). Finally, immunoreactive bands were detected using an LAS 4000 system (GE HealthCare, Barrington, Illinois, USA).

t-SNE and FlowSOM analysis

The flow cytometric data files were gated for singlet viable events.[53] Doublet cells and dead cells were removed using default parameters of Cytobank (V.10.6, California, USA). After the cleanup processes, multidimensional data were analyzed with the dimensionality algorithm t-SNE CUDA (t-distributed stochastic neighbor embedding compute unified device architecture) and the clustering algorithm FlowSOM. The density plot of t-SNE plots to reveal the NK cell population is an overlay of uncolored contour plots of CD45$^+$ cells and contour plots of highlighted cells colored by density.

Statistical analysis

All statistical calculations were performed using GraphPad Prism software V.9 (GraphPad Software, California, USA). The details of the statistical tests are indicated in the corresponding legends. Data are provided as mean±SD. P value<0.05 was considered statistically significant.

ORCID iDs
Seung Hee Choi http://orcid.org/0000-0002-8736-7969
Kyung-Soon Park http://orcid.org/0000-0002-0615-4313

REFERENCES

1 Kannan GS, Aquino-Lopez A, Lee DA. Natural killer cells in malignant hematology: A primer for the non-immunologist. *Blood Rev* 2017;31:1–10.
2 Liu S, Galat V, Galat Y, *et al*. NK cell-based cancer immunotherapy: from basic biology to clinical development. *J Hematol Oncol* 2021;14:7.
3 Löfstedt A, Chiang SCC, Onelöv E, *et al*. Cancer risk in relatives of patients with a primary disorder of lymphocyte cytotoxicity: a retrospective cohort study. *Lancet Haematol* 2015;2:e536–42.
4 Di Vito C, Mikulak J, Mavilio D. On the Way to Become a Natural Killer Cell. *Front Immunol* 2019;10:1812.
5 Shimasaki N, Jain A, Campana D. NK cells for cancer immunotherapy. *Nat Rev Drug Discov* 2020;19:200–18.
6 Huntington ND, Cursons J, Rautela J. The cancer-natural killer cell immunity cycle. *Nat Rev Cancer* 2020;20:437–54.
7 Liu E, Marin D, Banerjee P, *et al*. Use of CAR-Transduced Natural Killer Cells in CD19-Positive Lymphoid Tumors. *N Engl J Med* 2020;382:545–53.
8 Marin D, Li Y, Basar R, *et al*. Safety, efficacy and determinants of response of allogeneic CD19-specific CAR-NK cells in CD19$^+$ B cell tumors: a phase 1/2 trial. *Nat Med* 2024;30:772–84.
9 Gauthier L, Morel A, Anceriz N, *et al*. Multifunctional Natural Killer Cell Engagers Targeting NKp46 Trigger Protective Tumor Immunity. *Cell* 2019;177:1701–13.
10 Cózar B, Greppi M, Carpentier S, *et al*. Tumor-Infiltrating Natural Killer Cells. *Cancer Discov* 2021;11:34–44.
11 Pockley AG, Vaupel P, Multhoff G. NK cell-based therapeutics for lung cancer. *Expert Opin Biol Ther* 2020;20:23–33.
12 Muntasell A, Rojo F, Servitja S, *et al*. NK Cell Infiltrates and HLA Class I Expression in Primary HER2$^+$ Breast Cancer Predict and Uncouple Pathological Response and Disease-free Survival. *Clin Cancer Res* 2019;25:1535–45.
13 Liu P, Chen L, Zhang H. Natural Killer Cells in Liver Disease and Hepatocellular Carcinoma and the NK Cell-Based Immunotherapy. *J Immunol Res* 2018;2018:1206737.
14 Nersesian S, Schwartz SL, Grantham SR, *et al*. NK cell infiltration is associated with improved overall survival in solid cancers: A systematic review and meta-analysis. *Transl Oncol* 2021;14:100930.
15 Havel JJ, Chowell D, Chan TA. The evolving landscape of biomarkers for checkpoint inhibitor immunotherapy. *Nat Rev Cancer* 2019;19:133–50.

16 Ran GH, Lin YQ, Tian L, *et al*. Natural killer cell homing and trafficking in tissues and tumors: from biology to application. *Signal Transduct Target Ther* 2022;7:205.

17 Hydes T, Noll A, Salinas-Riester G, *et al*. IL-12 and IL-15 induce the expression of CXCR6 and CD49a on peripheral natural killer cells. *Immun Inflamm Dis* 2018;6:34–46.

18 Hodge DL, Schill WB, Wang JM, *et al*. IL-2 and IL-12 alter NK cell responsiveness to IFN-gamma-inducible protein 10 by down-regulating CXCR3 expression. *J Immunol* 2002;168:6090–8.

19 Carson WE, Giri JG, Lindemann MJ, *et al*. Interleukin (IL) 15 is a novel cytokine that activates human natural killer cells via components of the IL-2 receptor. *J Exp Med* 1994;180:1395–403.

20 Barlic J, Sechler JM, Murphy PM. IL-15 and IL-2 oppositely regulate expression of the chemokine receptor CX3CR1. *Blood* 2003;102:3494–503.

21 Burke JD, Young HA. IFN-γ: A cytokine at the right time, is in the right place. *Semin Immunol* 2019;43:101280.

22 Vivier E, Tomasello E, Baratin M, *et al*. Functions of natural killer cells. *Nat Immunol* 2008;9:503–10.

23 Choi SH, Kim HJ, Park JD, *et al*. Chemical priming of natural killer cells with branched polyethylenimine for cancer immunotherapy. *J Immunother Cancer* 2022;10:e004964.

24 Ko E-S, Choi SH, Lee M, *et al*. 25KDa branched polyethylenimine increases interferon-γ production in natural killer cells via improving translation efficiency. *Cell Commun Signal* 2023;21:107.

25 Lin Q, Rong L, Jia X, *et al*. IFN-γ-dependent NK cell activation is essential to metastasis suppression by engineered Salmonella. *Nat Commun* 2021;12:2537.

26 Yao X, Matosevic S. Chemokine networks modulating natural killer cell trafficking to solid tumors. *Cytokine Growth Factor Rev* 2021;59:36–45.

27 Brass A, Brenndörfer E. The Role of Chemokines in Hepatitis C Virus-Mediated Liver Disease. *IJMS* 2014;15:4747–79.

28 Inngjerdingen M, Damaj B, Maghazachi AA. Human NK cells express CC chemokine receptors 4 and 8 and respond to thymus and activation-regulated chemokine, macrophage-derived chemokine, and I-309. *J Immunol* 2000;164:4048–54.

29 Ye T, Zhang X, Dong Y, *et al*. Chemokine CCL17 Affects Local Immune Infiltration Characteristics and Early Prognosis Value of Lung Adenocarcinoma. *Front Cell Dev Biol* 2022;10:816927.

30 Cristiani CM, Turdo A, Ventura V, *et al*. Accumulation of Circulating CCR7+ Natural Killer Cells Marks Melanoma Evolution and Reveals a CCL19-Dependent Metastatic Pathway. *Cancer Immunol Res* 2019;7:841–52.

31 Ali TH, Pisanti S, Ciaglia E, *et al*. Enrichment of CD56(dim)KIR + CD57 + highly cytotoxic NK cells in tumour-infiltrated lymph nodes of melanoma patients. *Nat Commun* 2014;5:5639.

32 Kim J, Kim JS, Lee HK, *et al*. CXCR3-deficient natural killer cells fail to migrate to B16F10 melanoma cells. *Int Immunopharmacol* 2018;63:66–73.

33 Wendel M, Galani IE, Suri-Payer E, *et al*. Natural killer cell accumulation in tumors is dependent on IFN-gamma and CXCR3 ligands. *Cancer Res* 2008;68:8437–45.

34 Mayol K, Biajoux V, Marvel J, *et al*. Sequential desensitization of CXCR4 and S1P5 controls natural killer cell trafficking. *Blood* 2011;118:4863–71.

35 Correia AL, Guimaraes JC, Auf der Maur P, *et al*. Hepatic stellate cells suppress NK cell-sustained breast cancer dormancy. *Nature New Biol* 2021;594:566–71.

36 Liao Y-Y, Tsai H-C, Chou P-Y, *et al*. CCL3 promotes angiogenesis by dysregulation of miR-374b/ VEGF-A axis in human osteosarcoma cells. *Oncotarget* 2016;7:4310–25.

37 Vroon A, Heijnen CJ, Lombardi MS, *et al*. Reduced GRK2 level in T cells potentiates chemotaxis and signaling in response to CCL4. *J Leukoc Biol* 2004;75:901–9.

38 Ma Z, Zhang J, Wang L, *et al*. Expression and purification of recombinant human CCL5 and its biological characterization. *Protein J* 2022;41:337–44.

39 Zheng X, Wang Y, Wei H, *et al*. LFA-1 and CD2 synergize for the Erk1/2 activation in the Natural Killer (NK) cell immunological synapse. *J Biol Chem* 2009;284:21280–7.

40 Wu S-T, Sun G-H, Hsu C-Y, *et al*. Tumor necrosis factor-α induces epithelial-mesenchymal transition of renal cell carcinoma cells via a nuclear factor kappa B-independent mechanism. *Exp Biol Med (Maywood)* 2011;236:1022–9.

41 Deng S, Sherchan P, Jin P, *et al*. Recombinant CCL17 Enhances Hematoma Resolution and Activation of CCR4/ERK/Nrf2/CD163 Signaling Pathway After Intracerebral Hemorrhage in Mice. *Neurotherapeutics* 2020;17:1940–53.

42 Kremer V, Ligtenberg MA, Zendehdel R, *et al*. Genetic engineering of human NK cells to express CXCR2 improves migration to renal cell carcinoma. *J Immunother Cancer* 2017;5:73.

43 Li F, Sheng Y, Hou W, *et al*. CCL5-armed oncolytic virus augments CCR5-engineered NK cell infiltration and antitumor efficiency. *J Immunother Cancer* 2020;8:e000131.

44 Ng YY, Tay JCK, Wang S. CXCR1 Expression to Improve Anti-Cancer Efficacy of Intravenously Injected CAR-NK Cells in Mice with Peritoneal Xenografts. *Mol Ther Oncolytics* 2020;16:75–85.

45 Ralph CL. The pineal gland and geographical distribution of animals. *Int J Biometeorol* 1975;19:289–303.

46 Yan W, Jiang S. Immune Cell-Derived Exosomes in the Cancer-Immunity Cycle. *Trends Cancer* 2020;6:506–17.

47 Choi SJ, Cho H, Yea K, *et al*. Immune cell-derived small extracellular vesicles in cancer treatment. *BMB Rep* 2022;55:48–56.

48 Veerman RE, Güçlüler Akpinar G, Eldh M, *et al*. Immune Cell-Derived Extracellular Vesicles - Functions and Therapeutic Applications. *Trends Mol Med* 2019;25:382–94.

49 Kang Y-T, Niu Z, Hadlock T, *et al*. On-Chip Biogenesis of Circulating NK Cell-Derived Exosomes in Non-Small Cell Lung Cancer Exhibits Antitumoral Activity. *Adv Sci (Weinh)* 2021;8:2003747.

50 Aarsund M, Segers FM, Wu Y, *et al*. Comparison of characteristics and tumor targeting properties of extracellular vesicles derived from primary NK cells or NK-cell lines stimulated with IL-15 or IL-12/15/18. *Cancer Immunol Immunother* 2022;71:2227–38.

51 Choi SH, Cho HB, Choi J-H, *et al*. Nano-chemical priming strategy to enhance TGF-β resistance and anti-tumor activity of natural killer cells. *J Control Release* 2024;367:768–78.

52 Shannon P, Markiel A, Ozier O, *et al*. Cytoscape: a software environment for integrated models of biomolecular interaction networks. *Genome Res* 2003;13:2498–504.

53 Kotecha N, Krutzik PO, Irish JM. Web-based analysis and publication of flow cytometry experiments. *Curr Protoc Cytom* 2010;Chapter 10:Unit10.